論文・著書情報
Article・Book Information

Title	Development of snake-like robot ACM-R8 with large and mono-tread wheel
Authors	Hirotaka Komura, Hiroya Yamada, Shigeo Hirose
Citation	Advanced Robotics, Vol. 29, No. 17, pp. 1081-1094
Pub. date	2015, 9
Note	This is an electronic version of an article published in ADVANCED ROBOTICS, Vol. 29, No. 17, pp. 1081-1094, 2015. ADVANCED ROBOTICS is available online at: www.tandfonline.com. Article DOI: http://dx.doi.org/10.1080/01691864.2014.971054.
Note	このファイルは著者（最終）版です。 This file is author's final version.

To appear in *Advanced Robotics*
Vol. 00, No. 00, February 2014, 1–16

FULL PAPER

Development of Snake-like Robot ACM-R8 with Large and Mono-tread Wheel

Hirotaka Komura* , Hiroya Yamada and Shigeo Hirose

Tokyo Institute of Technology, 2-12-1 Ookayama, Meguro-ku, Tokyo;

(*v1.0 released February 2014*)

One of the important advantages of an active wheeled snake-like robots is that it can access narrow spaces which are inaccessible to other types of robot (such as crawlers, walking robots), since snake-like robots have an elongated, narrow body. Additionally, in areas with rubble, snake-like robots can traverse rough terrain and large obstacles since its body can conform to the terrain's contours. "ACM-R8" is a new snake-like robot which can climb stairs and reach doorknobs in addition to the features explained above. To fulfil these functions, the design of this robot incorporates several key features: joints with parallel link mechanism, mono-tread wheels with internal structure, force sensors and "swing-grousers" which were developed to improve step climbability. In this paper the design and control methods are described. Experiments confirmed high mobility on stairs and steps, with the robot succeeding in overcoming a step height of 600mm, despite the height of the robot being just 300mm.

Keywords: Active Cord Mechanism, Snake-Like Robot, Rescue Robot

1. Introduction

There is a demand for exploration inside buildings by robot, for the purpose of exploring dangerous environments or the automation of urban infrastructure inspection. As an example of exploration of a dangerous environment, disaster areas like the Fukushima daiichi nuclear power plant cannot be entered by humans because of the danger from radioactivity and rubble. In the inspection of urban infrastructure, exploration robots are also necessary since there is some terrain which is difficult for humans to enter because it is narrow or dangerous.

Inside buildings, there are various types of terrain which are difficult for robots: stairs, doors, rubble, etc. Additionally there may be some situations where the exploration robot must overcome some important or dangerous obstacles that cannot be touched. In this paper, a method to overcome such obstacles is proposed: a snake-like robot named " ACM-R8 "(Fig.1).

Snake-like robots are researched in all over the world and various types of snake-like robots have been developed. Our laboratory also have been researching them for a long time and have developed some models[1–3]., etc., since we believe that snake-like robots can adapt to various situations[4].As a locomotion mechanism, they are thought to be able to overcome various terrain since in nature snakes inhabit trees, sand, under water, etc. Additionally, the body can also be used as a robot arm by using its multiple DOF. A related study on a snake-like robot, the " Modular snake robot "[5] realizes various motion of snakes, especially tree climbing, and "OT-4 " [6] demonstrates excellent mobility on rough terrain.

*Corresponding author. Email: komura.h.aa@m.titech.ac.jp

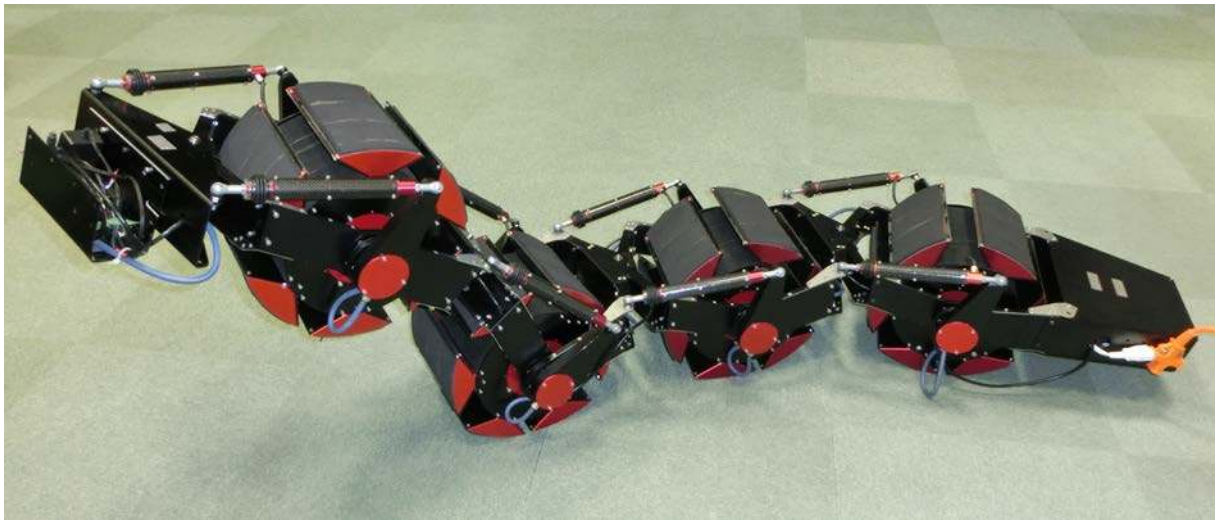

Figure 1. ACM-R8

The ACM-R4 series[7–9] equip active wheels on every module in addition to active joints. These wheels allow the robot to produce thrust force even if the locomotion method using the active joints cannot be used, for example in a narrow and straight passage. In the experiment to climb a single step, these robots could overcome a single step whose height was almost 3 times higher than their height when they are on a flat plane. ACM-R4.1[8] and ACM-R4.2[9] equip active wheels, and utilize terrain adaptive control by using torque sensors. These robots have shown excellent performance on rough terrain with active wheels and terrain adaptive control.

But these active-wheeled snake-like robots cannot climb stairs, since their size is too small. Additionally these robots cannot operate doors, since their bodies are too short to reach door knobs. The ACM-R8 is developed to solve these problems by using enlarged wheels and some unique mechanisms.

One the other hand there are some locomotion methods in robots other than snake-like robots. Generally these methods can be classified into wheel, crawler, walking and flying types.

Wheel type performs with high energy efficiency and speed, but this type is not suitable for rough terrain, since the step climbability is worse than other types, and this type tends to get stuck on obstacles. Active wheeled snake-like robot uses the wheel, but it is classified as separate from the wheel type, since the snake-like robot possesses redundant active joints and wheels.

The crawler type robots show high mobility on the rough terrain, since the area of surface generating the propulsive force is large. Quince [10] developed in CIT, and PackBot [11] developed in iRobot Corp. are famous for conducting exploration inside the reactor buildings of the Fukushima nuclear power plant. These robots show very high mobility in such an uneven environment, since they equip sub-crawlers.

The walking type robots show high suitability for rough and uneven terrain, since these robots can select the ground contact point, although their control systems are complicated. A quadruped walking robot developed in TOSHIBA Corp.[12] was also used in Fukushima nuclear power plant. This robot can climb up and down the steep and narrow stairs in the reactor buildings.

Flying robots can move three-dimensionally regardless of obstacles. This is their key advantage that no other robots have. On the other hand, the disadvantage of flying robots is the limited operating time and relatively small payload. Pelican [13] is quad-rotor robot, which can generate a three-dimensional map of the inside of a building.

The crawler type and walking type can perform with high mobility on rough terrain or stairs, but these types cannot pass through narrow passages, for example gaps in rubble, pipes. Additionally the crawler cannot get over obstacles without touching them. The flying type can get over all ground obstacles, but this type robot cannot operate door knobs.

ACM-R8 can climb stairs, move over rough terrain, and go through narrow spaces since this robot is smaller than the other types of robot. Additionally, we believe that this robot can reach and operate door knobs with some additional devices. In this paper the mechanism and the result of mobility experiment is described.

2. Overview of ACM-R8

As shown below, there are four design requirements for the ACM-R8.

- Stair climbability
- Able to reach door knobs
- Water proof system
- Reduction of width and height compared with other types of survey robots

To fulfil these points, ACM-R8 incorporates the next three features.

- Thin body with high ground clearance
- Larger wheel than previous models
- Torque measurement system for terrain adaptation

2.1 *The Layout of the wheel and the body*

One of the problems of the ACM-R4.1 is getting stuck as shown in Fig.2. This situation was caused by contact between the trunk and the edge of the obstacle, and reduced the thrust force since the wheel lost contact with the ground. To solve this problem, in the development of the ACM-R4.2, the wheels on the yaw joints are removed, and a thinner trunk was achieved as shown in Fig.4(a). But this solution was not enough to avoid the contact completely.

To improve this problem, the trunk of the ACM-R8 is located higher than the radius of the wheels, as shown in Fig.4(b). And the wheel of the ACM-R8 is wide and mono-tread type.Considering a tall and thin obstacle like Fig.3, the previous style is likely to get stuck as shown in Fig.3(a). On the other hand the mono-tread style does not get stuck easily since the surface generating traction exists in the center of the wheels as shown in Fig.3(b).This mono-tread type has another useful feature: the large space inside the wheel. The motor driving the yaw joint was moved and placed inside the wheel. Thus the yaw joint can be waterproofed more easily.

Additionally, to drive the yaw and pitch axis by the in-wheel motors, a parallel mechanism is used as a joint mechanism. This parallel mechanism performs with a better power to weight ratio than a serial mechanism, which was used in previous models. This feature of parallel mechanism is described in detail in chapter 3.1.

2.2 *The minimum required wheel diameter*

When an active wheeled snake-like robot climbs stairs, the robot may get stuck on the edges of steps and fall into a state where it is unable to climb up. Enlargement of the wheels is one way to solve this problem, since the larger the radius of wheels becomes, the longer the distance between edge and trunk becomes. At the same time this indicates that there is a limitation related to the height of one step.

This limitation was experimented with a scale model of stairs as shown in Fig.5. In this experiment, the ACM-R4.2 was equipped with grouser wheels and was used as a small model. This grouser wheel was prepared for this experiment, and the ratio of the grouser wheel diameter and the wheel interval were set to be equal to the ratio of the wheel diameter and the wheel interval of the ACM-R8. And this small stair possesses an inclination of 42 degrees and a changeable

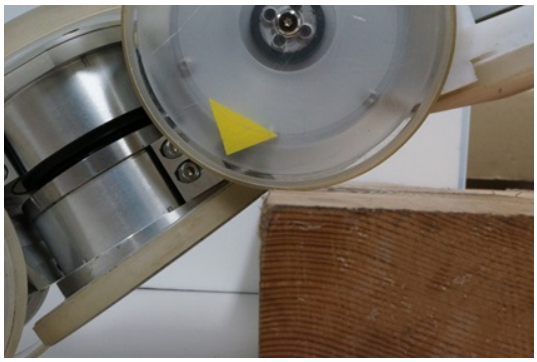

Figure 2. Stuck of ACM-R4.1 on step

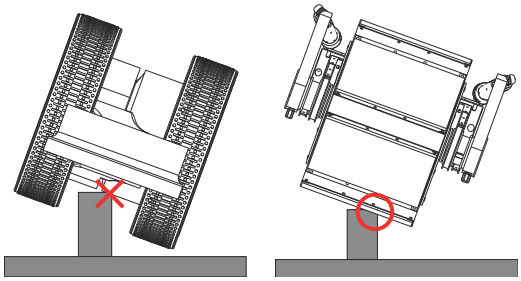

(a) ACM-R4.2 (b) ACM-R8

Figure 3. Comparison of ACM-R4.2 and ACM-R8 of front view (a) The trunk contacts with the obstacle and the robot gets stuck. (b) The wheel contacts with the obstacle and the robot can move.

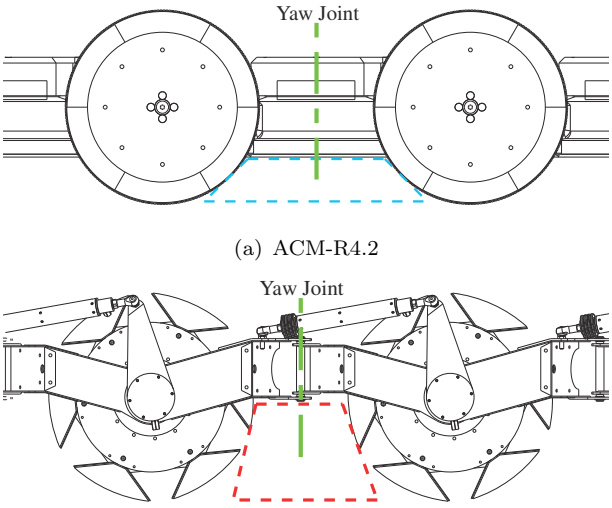

(a) ACM-R4.2

(b) ACM-R8

Figure 4. Comparison of ACM-R4.2 and ACM-R8 of side view (a) The space under the trunk is slightly small (b) The trunk is placed higher than the wheel radius

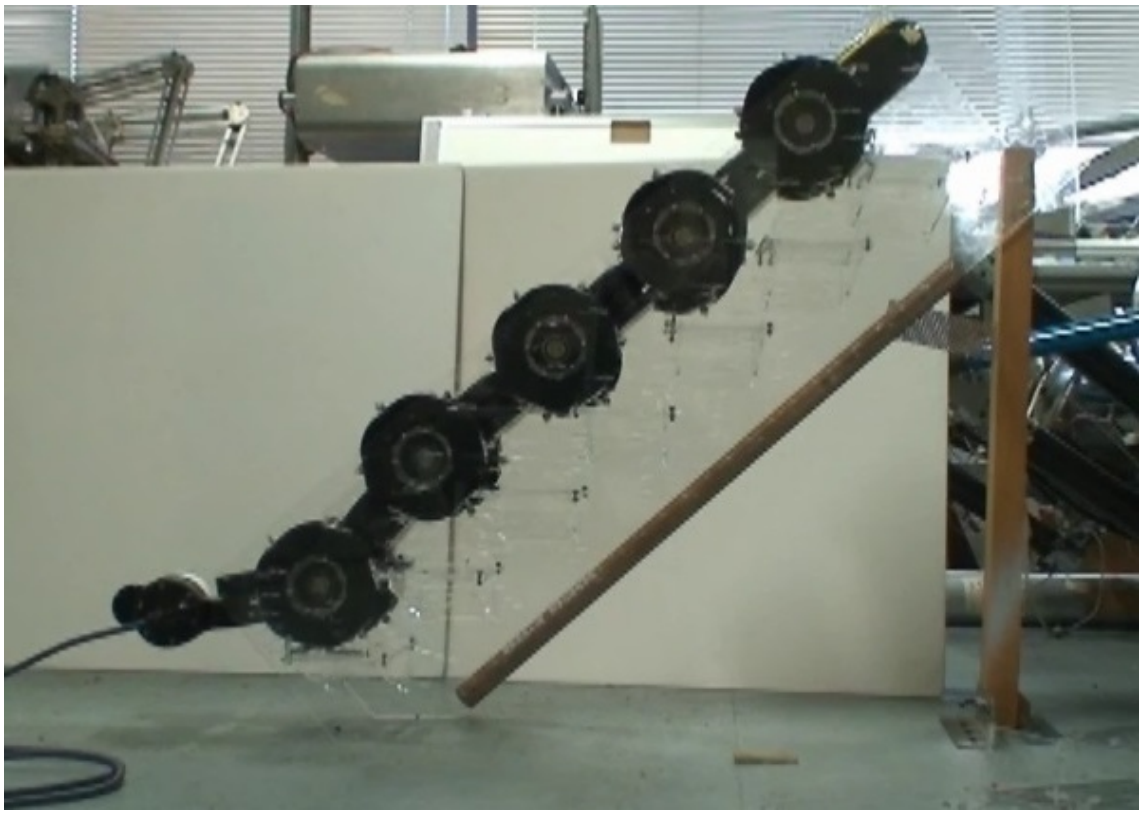

Figure 5. Experiment with scaled model

Table 1. Specification of ACM-R8

	Whole(4 units)	Single unit
Length	2010mm	440mm
Width	360mm	360mm
Height	300mm	300mm
weight	36.5kg	8.5kg
Total output of motors	960W	240W
Pitch range	-	□ 90 □
Yaw range	-	□ 45 □
Pitch torque	-	100Nm
Yaw torque	-	100Nm
Pitch speed	-	7.3rpm
Yaw speed	-	7.3rpm
Wheel torque	32Nm	-
Wheel velocity	0.4m/s(24.2rpm)	-
Turning radius	0.53m	-

step height.

The grouser wheel was 136mm diameter, and the robot climbed 90.7mm height steps, but failed to climb 108.8mm height steps. This result shows that the robot can climb with wheels whose diameters are larger than one and half times the height of the steps. From this result the wheel diameter of the ACM-R8 was decided to be 300mm, since the target of the ACM-R8 is a stair whose inclination is 42 degrees and whose step height is 200mm.

2.3 *Force sensor for measuring torque*

The ACM-R8 has a torque measuring mechanism installed since the effectiveness of torque measurement for terrain adaptation control was confirmed in previous research[8, 9]. With torque sensing, admittance control for the joints can be realized. The admittance control is one way to bend the trunk along the terrain automatically. This terrain adaptation increases the number of wheels in contact with ground, so the robot can get higher traction with this control. A further feature of torque measurement is that it can measure all external forces in the normal direction of the trunk, since it measures the internal force load to the joints.

3. Design of ACM-R8

The basic structure of the ACM-R8 is a modular robot, the same as other ACMs. One module (shown in Fig.6) incorporates a joint with 2 DOFs and one wheel. Thus each module has 3 DOFs. The joint mechanism has two force sensors installed for measurement of the load torque in the joint. The features of this module are the large, wide wheel and the simple frame with good ground clearance. The specification of the robot is shown in Table.1.

3.1 *The parallel link mechanism of the joint*

The mechanism shown in Fig.7 is a parallel link mechanism with 2 DOFs, in the pitch and yaw axes. The motors are placed at the base of the A links, and the C link is connected to the front unit. Driving both A links in the same direction causes the joint mechanism to move around the pitch axis. On the other hand, driving A links in opposite directions causes the joint to move around the yaw axis.

This mechanism can move with a large range of pitch angle. This large range of motion allows the snake-like robot to bend the trunk at a right angle, and makes it easier to place the head in a high position. Thus this mechanism is used for the joints of the ACM-R8 since there is a requirement to reach door knobs.

Additionally, there are two features other than the wide range of motion in this parallel link

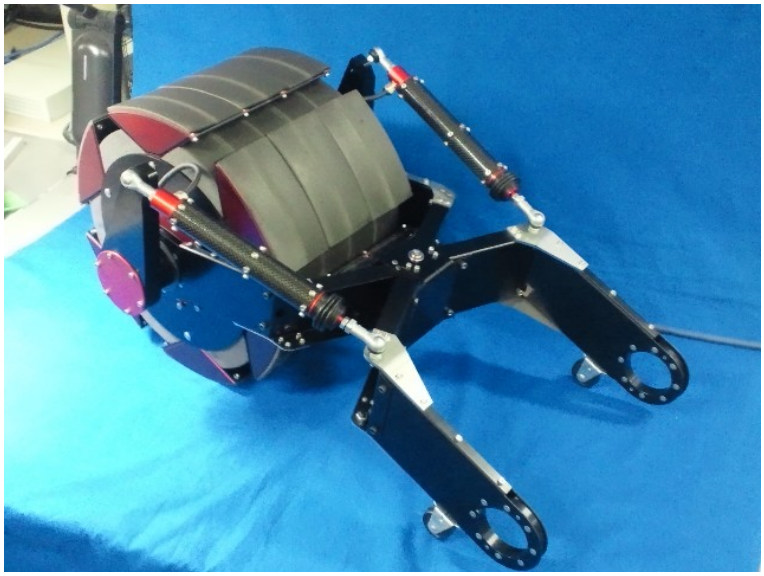

Figure 6. One module of ACM-R8

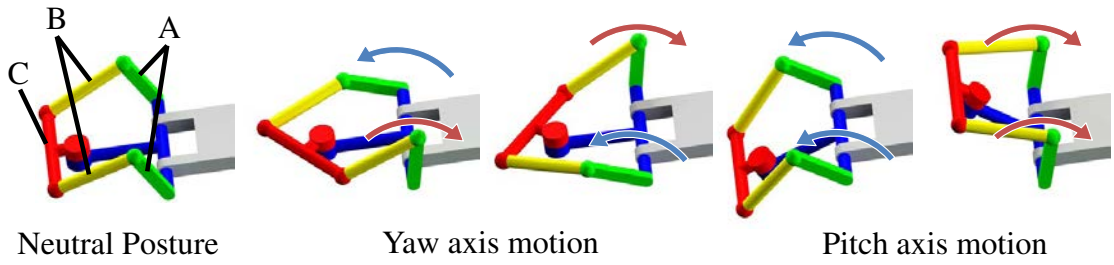

Figure 7. Schematic view of the joint

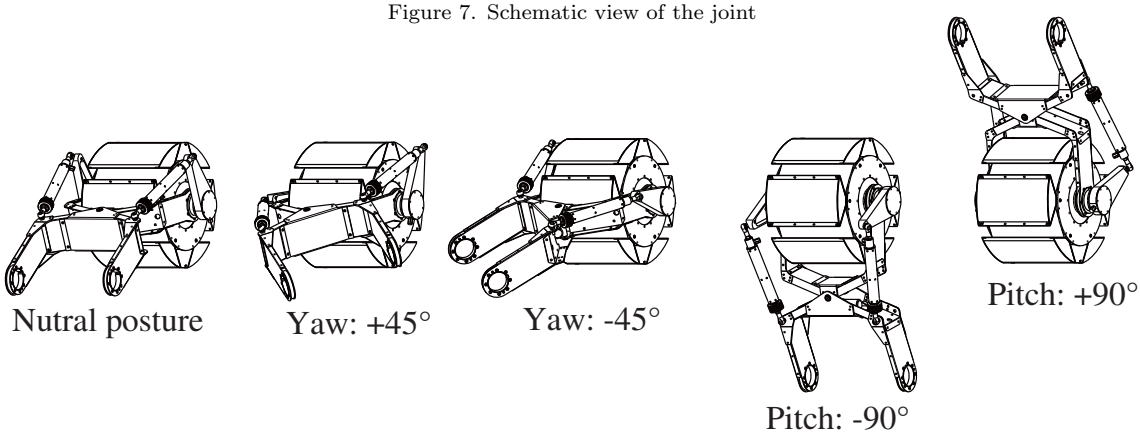

Figure 8. Motion range of the joint

mechanism. The first one is the placement of the motors. With this mechanism the motors can be placed at the base of the mechanism, which is located inside the wheel. This means that the points which need to be are reduced as mentioned above, with only two points (the left and right sides of the wheel) need to be waterproofed. The second is that the power to weight ratio of this mechanism is higher than the power to weight ratio of the serial link mechanism. As shown in Fig.7, both motors are driven when the mechanism moves around the yaw or pitch axis. The motion of the joint is shown in Fig.8. As shown in the figure, the range of motion of the yaw axis is $\pm 45°$, and the range of the pitch axis is larger than $\pm 90°$.

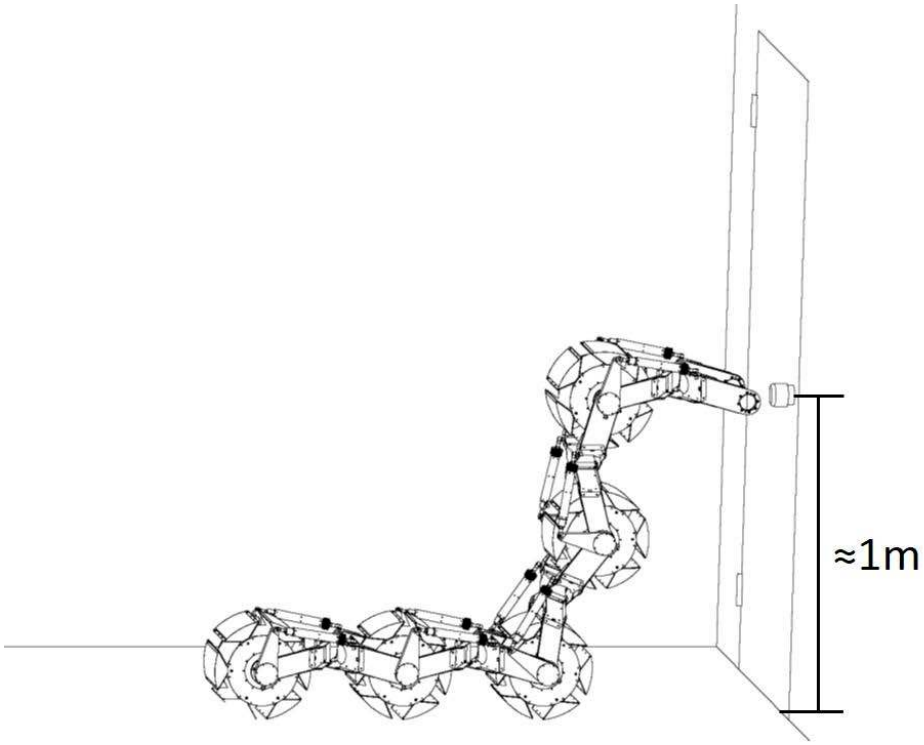

Figure 9. Reaching doorknob image

3.2 *Doorknob reachability*

One of the requirements of the ACM-R8 is being able to reach doorknobs and operate them. Thus, the trunk must be able to reach doorknobs, which are located at a height of around 1m. The motors and the speed reducers of each joint are selected to satisfy this. And, like Fig.9, raising more than 2 modules make it possible to reach 1m height, since the interval of each joint is 440mm, and the wheel radius is 150mm. In this case the maximum load torque to the joint was found when raising 2 modules. This can be calculated by the next expression, where m is the mass of one module, and l is the interval of each module.

$$2mg \times l = 2 \times 8.5[kg] \times 9.8[m/s^2] \times 0.44[m] = 73.4[Nm] \tag{1}$$

As shown in Table.1, the output torque of the joint is enough to satisfy this motion. But, at the moment, the robot cannot realize this motion since only 4 modules have been developed. Thus, as a future plan, making another one module is scheduled.

3.3 *Force-sensor*

The torque measurement mechanism of the ACM-R8 is composed with the parallel link mechanism of the joint by installing two linear force sensors. The force sensors are located in the B links in Fig.7. The sectional view of a force sensor link is shown in Fig.10. This sensor is composed with a spring and a linear magnet encoder, and a linear link. The load for this spring is only a linear force since both sides of this link have spherical joints. The load can be measured by detecting the spring deformation using the linear magnet encoder. The linear magnet encoder is AS5306A-ATSU from Austriamicrosystems Corp., and its resolution is 15μm. The model number of the spring is 53-1635 in SAMINI Corp., and its spring constant is 98.8N/mm. Thus the resolution of the force sensor is 1.8N. From the length and the angle of each link and

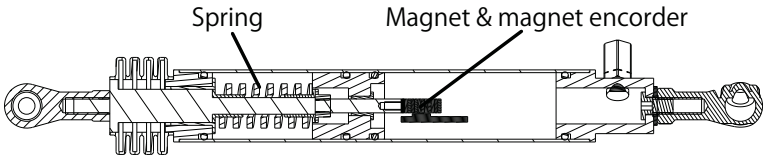

Figure 10. Sectional view of force-sensor

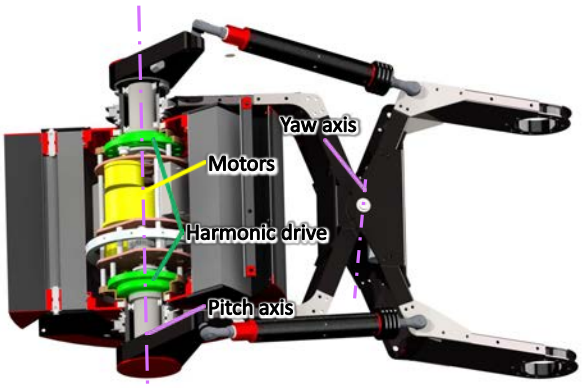

Figure 11. Inside of the wheel

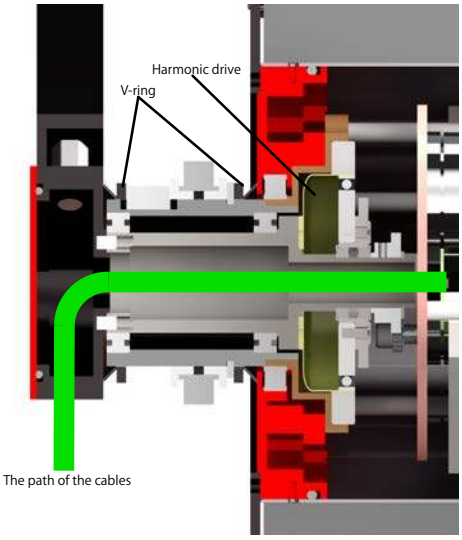

Figure 12. The end of the wheel

the information of the forces in the left and right sensors, the load torque of the joint can be calculated. The stretching part of this sensor is covered by bellows for waterproofing. This force sensor has a certain elasticity since the spring is installed. This elasticity reduces the precision of position control, but in this case this feature is not so bad, since it reduces the impulsive force of the actuators, and it gives some adaptability to the snake-like robot trunk.

3.4 *Detail of the inside of the wheel*

Fig.11 is a CAD model of the inside of the wheel. There are two harmonic drives, three motors, one microcontroller and three motor drivers inside each module. The harmonic drives are located at both sides of the wheel, and connected to the motors by one-step spur gears. The harmonic drives are used for driving the joint link mechanism. The harmonic drives are CSD-25 from Harmonic drive systems Corp., and the motors are EC45flat from MaxonMotor Corp. With these actuator units, the joint can lift two of the modules as mentioned in 3.2. There is a motor at the center of the unit, and this motor is used for driving the wheel. This motor is also from MaxonMotor Corp., and the model number is EC60flat. This wheel can lift up two modules. The microcontroller is a TITechSH2 Tiny Controller from Hibot Corp. The sectional view of left and right sides of the wheel are shown in Fig.12. The path of the cable goes through the center of the shafts. V-rings are attached to the sliding parts for waterproofing. In each module the sliding part exists only on both sides of the wheel.

3.5 *Swing-grouser*

A new wheel grouser, named Swing-grouser (Fig.13) was developed to improve the step climbability of each wheel. This mechanism was confirmed to climb a step higher than the radius of the wheel. In this wheel fan shape grousers are attached instead of the normal protruding grouser. These grousers are attached to the wheel by a passive rotation axis, and keep their

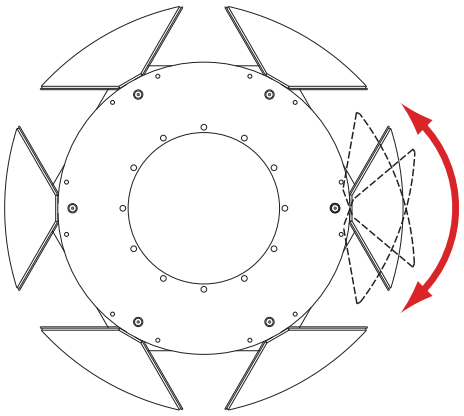

Figure 13. Swing-grouser

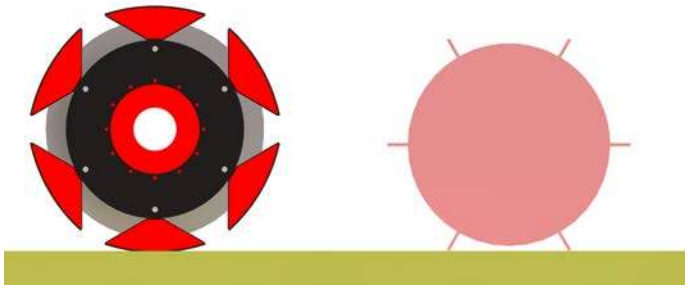

Figure 14. Comparison of swing-grouser and normal grouser on flat

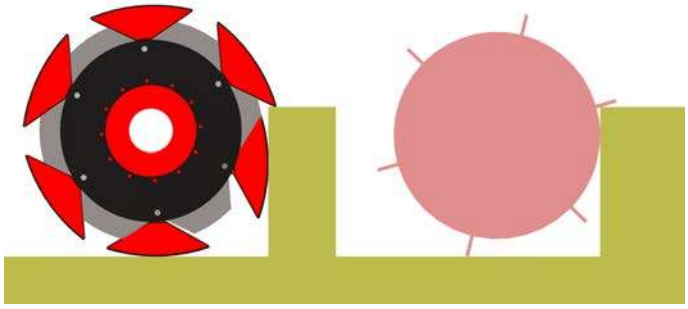

Figure 15. Comparison of swing-grouser and normal grouser on step

neutral position by elastic sponge. Thus, with this elasticity the swing-grousers keep their neutral position with no external forces. But when some external forces occur by hitting obstacles, the grouser moves around like shown the arrow in Fig.13.

Fig.14 and Fig.15 is a comparison between the swing-grouser and the normal grouser. On the flat ground shown in Fig.14, the shape of the wheel equipped with the swing-grousers is more circular than the shape of the wheel equipped with the normal grousers. Thus we consider that the energy efficiency of the swing-grouser is higher than the efficiency of a normal grouser, since the vertical vibration is reduced by the more circular shape. On a single step which is higher than the radius of the wheel, shown in Fig.15, the normal grouser hits the edge of the step. In this situation, the friction force must be enough large to climb up the step, otherwise the wheel falls and cannot climb. But the swing-grouser hits the step and deforms, thus the next grouser hooks on the top of the step even if the step height is higher than the radius of the wheel. This system makes it possible to climb a higher step than the normal one can climb.

In brief, we consider that the swing-grouser has higher step climbability and higher energy efficiency than a normal grouser wheel. All of the wheels of the ACM-R8 equip this swing-grouser since this element is expected to improve the step climbability of the snake-like robot. The step climbability of the swing-grouser was experimented with a prototype of one module of the ACM-R8. The robot succeeded in climbing a 189mm height step with 150mm radius wheel as shown in Fig.16. From this result, it was confirmed that the swing-grouser can climb a step whose height is higher than the radius of the wheel.

At the moment, the shapes or elasticity of swing-grouser has not been optimized. Thus, actually the parameters of the swing-grouser equipped with the ACM-R8 were decided with some uncertainty. We believe that an optimization of the shape and the elasticity will improve the step climbability and the energy efficiency of the swing-grouser.

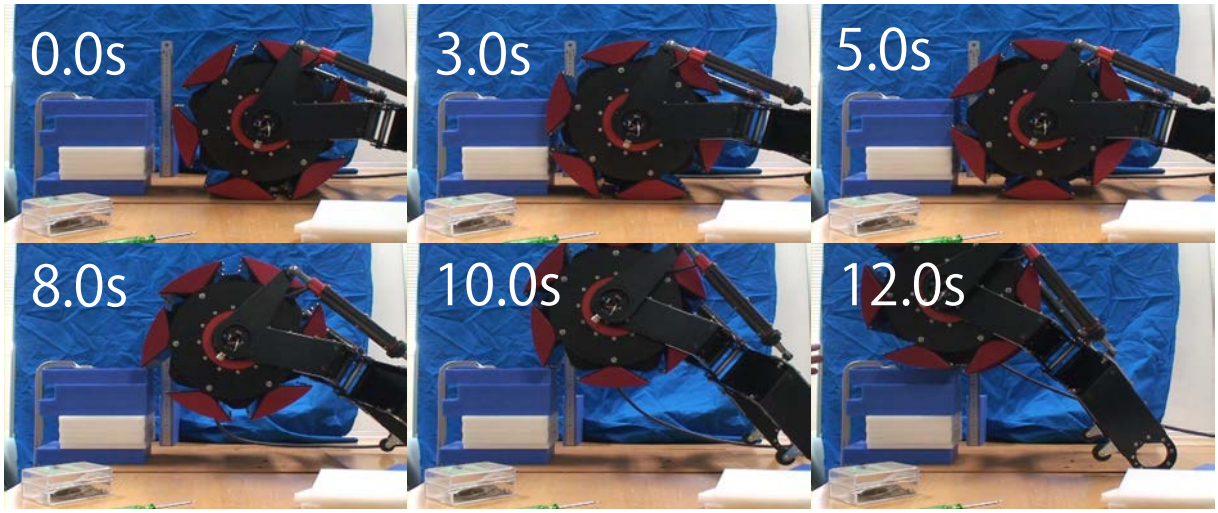

Figure 16. Experiment of swing-grouser

3.6 *Electrical system*

The electrical power and the communication of the ACM-R8 is supplied by wire, in order to reduce the weight of the robot and increase the reliability in the disaster area or indoor environment, where there are many obstacles which may block radio waves, for example walls, metal and water. Fig.17 shows the electrical power and communication system of the ACM-R8. Each unit converts AC100V to DC24V for driving their motors by AC-DC converters since the standard household voltage in Japan is 100 V. As a result, the robot can be used in Japan without any special power supply unit. At the same time this power supply line can be used as a communication line between the controlling PC and the robot by using PLC communication with PLC adapters, BL-PA304 from Panasonic Corp. These adapters are useful for the ease of installing Ethernet devices, for example network cameras.

In the tail of the robot, the signal on the Ethernet is converted to RS232C by XPort from LANTRONIX Corp., and connected to the SH2 microcontroller board. The microcontrollers in the tail and every modules communicate with each other via CAN Bas, and these microcontrollers control the motor drivers in each module.

The data sent from the PC to the microcontrollers are the target value of the joint angles and wheels, and the spring constant for admittance control. On the contrary, the measured angles of the joint, load torque, and current of motors are sent from the microcontrollers to the PC. Thus the calculation for deciding the target value is done on the PC, and the microcontrollers calculate the position control of the joints and velocity control of the wheels in each module.

Each module includes hall sensors, potentiometers and force sensors. The hall sensors are equipped in the motors, and used for position control. But hall sensors cannot measure the absolute position, thus the potentiometers are used during initialization. The force sensors are used for admittance control, as explained in chapter 3.3.

4. Control system of the ACM-R8

Since the hardware system of the ACM-R8 is similar to the ACM-R4.2, the control system of ACM-R8 was developed using the knowledge of previous work.

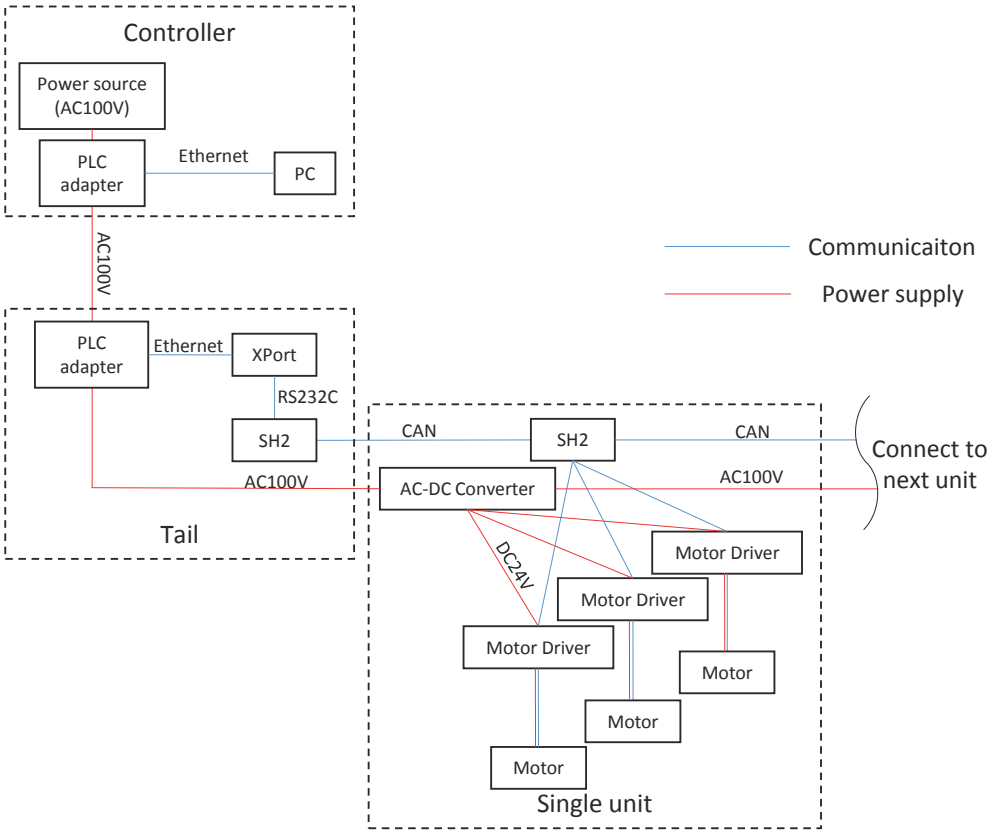

Figure 17. Electorical system of ACM-R8

4.1 *Approximation to continuous curves*

In the system of the ACM-R8, approximations to continuous curves[14] is used for deciding the joint angles. This is a method to control the trunk of snake-like robots with a continuous curve. By using the continuous curves various motions of a snake-like robot can be expressed generally, regardless of the mechanism and size of the robot. In this paper we describe how to convert between the continuous curve and the real robot model, and how to achieve lateral rolling, as well as how to move forward by shifting the joint angles.

In this method, the snake-like robot is considered as a continuous space curve with vertical and horizontal curvature. This continuous curve is approximated to a discrete model in the way explained below. In controlling the robot the joint angles of the discrete model are applied since the joints of the real robot are discrete.

The pitch and yaw angles of the joint, θ_{pi} and θ_{yi} , where i is a number of the joint, are calculated by eq.2. This is how the continuous model is approximated to the discrete model. L is the length of the continuous curve, $\kappa_p(s)$ and $\kappa_y(s)$ represent the vertical and horizontal curvature distribution function where $s(0 \leq s \leq L)$ is a length from the end of the curve.

$$\begin{cases} \theta_{pi} = \int_{(i-1/2)l}^{(i+1/2)l} \kappa_p(s)ds \\ \theta_{yi} = \int_{il}^{(i+1)l} \kappa_y(s)ds \end{cases} \tag{2}$$

Lateral rolling[1] can be performed by changing the vertical and horizontal curvature distribution function by eq.3. ψ is the change quantity of the lateral rolling angle per controlling cycle.

$$\begin{pmatrix} \kappa_{pnew}(s) \\ \kappa_{ynew}(s) \end{pmatrix} = \begin{pmatrix} \cos(\psi) & -\sin(\psi) \\ \sin(\psi) & \cos(\psi) \end{pmatrix} \begin{pmatrix} \kappa_p(s) \\ \kappa_y(s) \end{pmatrix} \tag{3}$$

Forward movement is described by eq.4, where v is the moving distance par controlling cycle. When the robot moves forward, the curvature distribution function is recalculated. Specifically, the curvature distribution function is offset backward by v, and new curvature values $\kappa_{ptarget}$ and $\kappa_{ytarget}$ are substituted. At the same time, the wheel gets the velocity target same as v. Moving backward can be realized in the same manner.

$$\begin{cases} \kappa_{pnew}(s) = \kappa_p(s+v) \\ \kappa_{ynew}(s) = \kappa_y(s+v) \end{cases} \quad (s \leq L - (v+l)) \\ \begin{cases} \kappa_{pnew}(s) = \kappa_{ptarget} \\ \kappa_{ynew}(s) = \kappa_{ytarget} \end{cases} \quad (L - (v+l) < s \leq L) \tag{4}$$

Additionally, moving backward can be realized in the same way.

4.2 *Admittance control*

The admittance control, whose effectiveness for rough terrain was confirmed in previous research, is used for controlling the joints of the ACM-R8. When the admittance control is applied, the target angle of the joints is changed by the spring constant set by the operator and the external torque to the joints as shown in Fig.18. The actual target angle θ' can be calculated with eq.5, where T_{load} is an external torque for the joint, and K is the spring constant.

$$\theta' = \theta - \frac{T_{load}}{K} \tag{5}$$

When the robot moves over a groove like Fig.19, the robot bends along the groove automatically by the admittance control. The thrust force can be generated more reliably on rough terrain, since this effect increases the number of wheels contacting the ground. The advantage of admittance control is to be able to change the elasticity according to different situations. For example, when overcoming a large groove, the joints must be rigid since an elastic trunk tends to fall into the groove, and make it difficult to get over. On the other hand, elastic joints are necessary for getting through rough terrain, since a rigid trunk cannot follow complicated terrain. To achieve excellent performance in both situations, the elasticity of the trunk must be controllable. Furthermore, admittance control makes it possible to realize the elastic pitch axis and rigid yaw axis at the same time, by setting a different elasticity for each axis, even though the joint mechanism is a parallel mechanism.

5. Mobility experiment

5.1 *admittance control*

Comparative experiments between normal position control and admittance control which were explained above were conducted. As shown in Fig.20, when the robot was in position control (Fig.20(a)) its head unit was lifted up with other units, but in case of admittance control (Fig.20(b)) the head unit hung down since the second unit measured the torque produced by the gravity force and changed the target position.

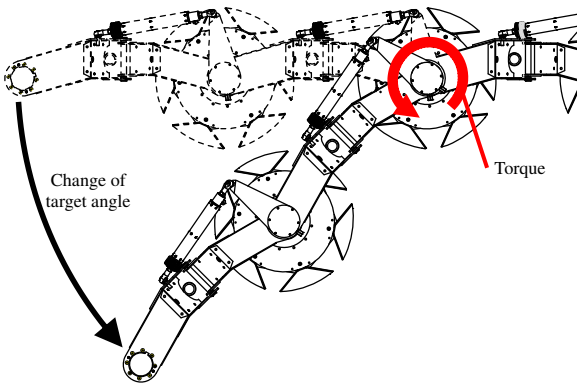

Figure 18. Motion of admittance control

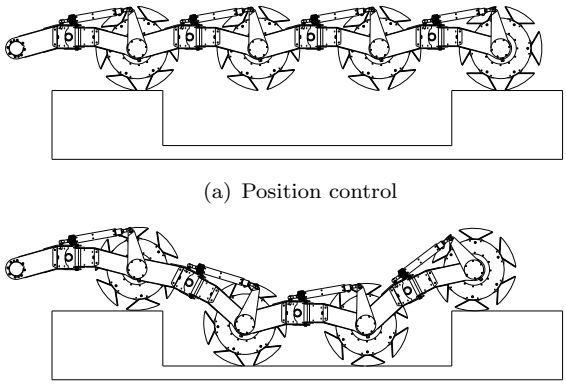

(a) Position control

(b) Admittance control

Figure 19. Image of position control and admittance control

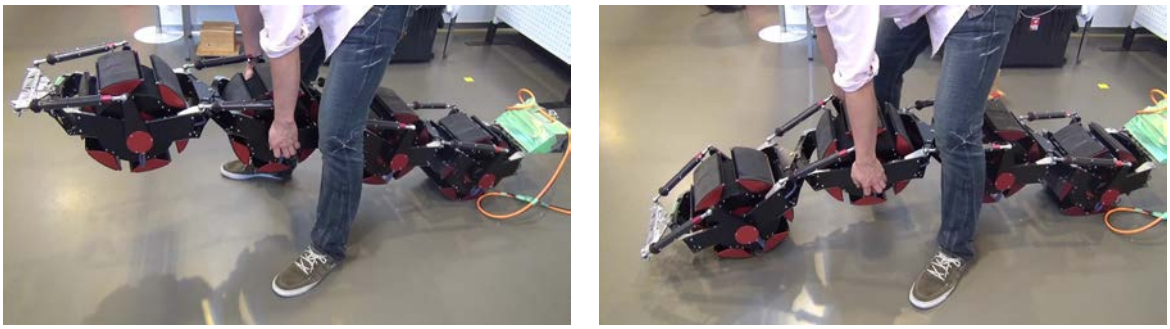

(a) Position control

(b) Admittance control

Figure 20. Image of admittance control and position control

Figure 21. Getting over the block and turning

5.2 *Basic motion*

As shown in Fig.21, the ACM-R8 succeeded to move forward with its active wheels, getting over the 10cm wooden block and moving forward avoiding the pole. In this experiment admittance control was used for each pitch axis of the joint to realize some elasticity. While getting over the block, controlling the pitch axis was not necessary since the trunk follows the shape of block automatically by admittance control. The advantage of terrain adapting by admittance control

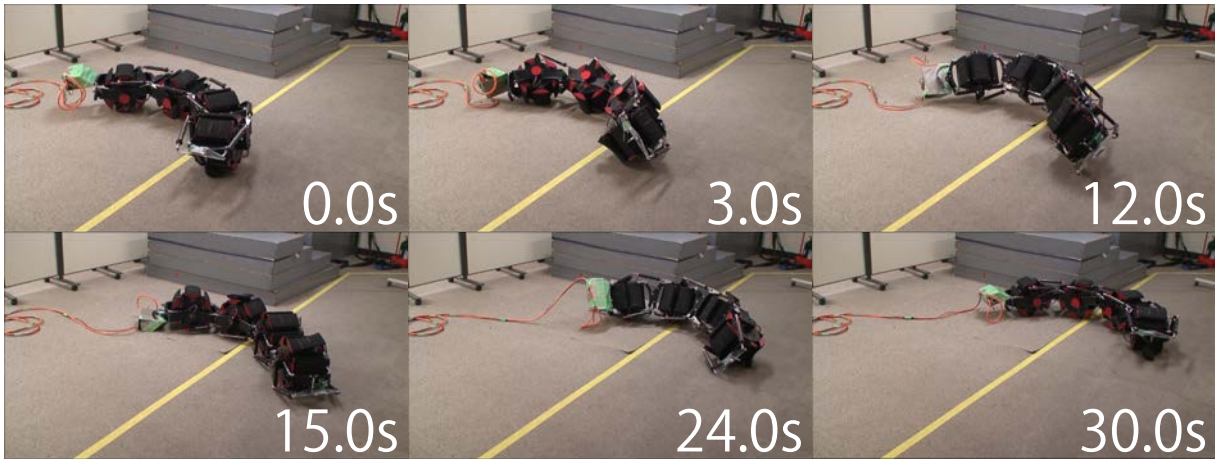

Figure 22. Lateral rolling

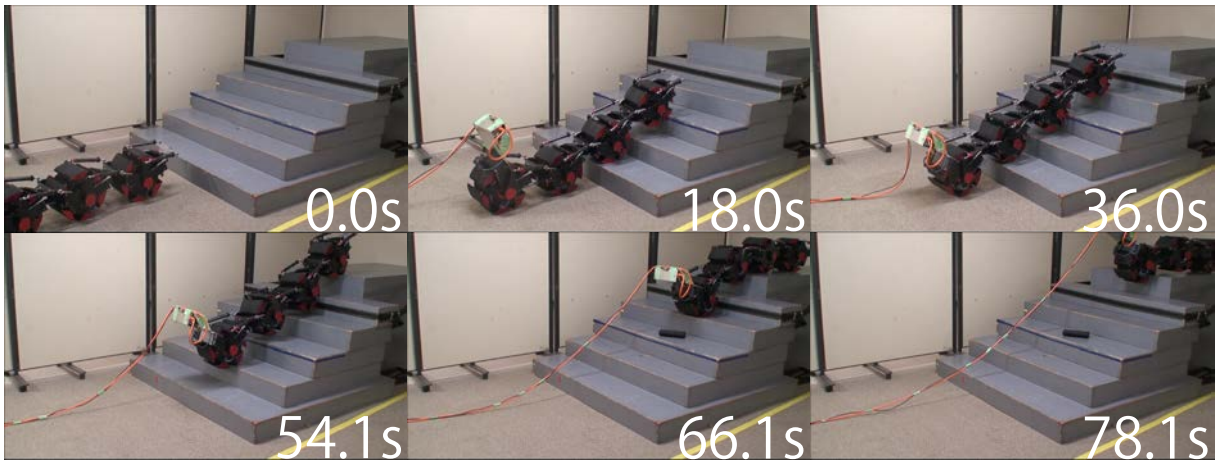

Figure 23. Climbing stair

was confirmed with this experiment. In this experiment the average velocity was about 0.1m/s.

5.3 *Lateral rolling*

The ACM-R8 succeeded in lateral rolling on a flat surface as shown in Fig.22. At 0.0s, each joint was tilted 45 □ in the yaw axis, and straight in the pitch axis. The joint angles were changed in the way described in chapter 4.1. In this experiment, the angular velocity was about $12°/sec.$ In this way, the same as other ACMs, ACM-R8 can move sideways without turning in the yaw axis, and return to the original posture even when the robot tumbles.

5.4 *Stair climbing experiment*

A stair climbing experiment was conducted with the robot as shown in Fig.23. The height of this stair was 150mm, and the inclination was 30°. Admittance control was used in the pitch axis, to adapt the trunk to the stairs' unevenness. In this experiment, the average velocity was 0.05m/s, to reduce the risk of breakdown. As shown in some of the pictures of Fig.23, the swing grouser caught the edge of the steps. The round surface of the swing-grouser slipped with the edge of the steps, but while the edge of swing-grouser caught the step, the robot could climb without slipping. It was confirmed that the swing-grouser made it easy to climb the stairs.

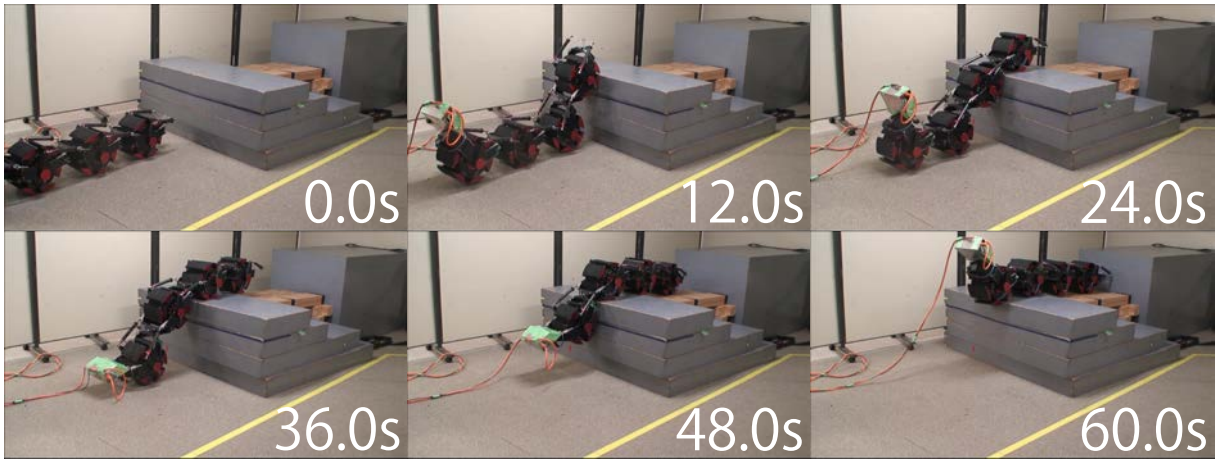

Figure 24. Climbing 60cm step

After this experiment, climbing down the stair was tested successfully. The ACM-R8 succeeded to climb both up and down the stairs.

5.5 *Single step*

Fig.24 shows the single step experiment. In this experiment, the robot climbed a step of height 600mm. As well as the stair climbing experiment, admittance control was used for each pitch axis in this experiment. Additionally, the same as the stair climbing experiment, while the swing-grouser caught the edge of the step, the robot could move without slipping. Moreover, the robot could climb a step of height 450mm as well, and succeeded to get off from each step, without any collisions and without falling.

6. Conclusions

In this paper, a new snake-like robot named ACM-R8 was proposed, and its design and control system were described. Its basic performance was confirmed in some experiments. At the present stage, the robot succeeded climbing a simple set of stairs and climbing a 60cm height step. Especially, for climbing a high step, excellent results were achieved.

As a future plan, attaching cameras is scheduled in order to control without watching the robot directly and improve its practicality. Furthermore, equipping a gripper and one more module are scheduled to achieve the reachability and operability of door knobs.

Also a new mechanical element named Swing-Grouser is proposed in this paper. The wheel equipped with Swing-Grousers succeeded in climbing steps higher than the wheel s radius. In this paper the swing-grouser is used for a snake-like robot, but it can be used for many wheeled robots. But the advantages of the swing-grouser have not been shown clearly, since no comparative experiments were done among the swing-grouser and normal grouser, or other types of wheels. At the same time the shape and elasticity of swing-grouser have not yet been optimized. Thus, as a future plan, an analysis and comparative experiments about the energy efficiency and step climbability of the swing grouser should be done.

References

[1] M. Mori, S. Hirose, Y. Zhang, M. Schervish, and H. Choset, “Three-dimensional serpentine motion and lateral rolling by active cord mechanism acm-r3,” in *in Proc. 2002 IEEE/RSJ Int. Conf, on*

Intelligent Robots and Systems, 2002, pp. 829–834.

[2] H. Yamada, S. Chigisaki, M. Mori, K. Takita, K. Ogami, and S. Hirose, "Development of amphibious snake-like robot acm-r5," in *Proc.ISR2005*, 2005, p. TH3C4.

[3] T. Ohashi, H. Yamada, and S. Hirose, "Loop forming snake-like robot acm-r7 and its serpenoid oval control," in *IROS*. IEEE, 2010, pp. 413–418.

[4] S. Hirose, *Biologically inspired robots: snake-like locomotors and manipulators*, ser. Oxford science publications. Oxford University Press, 1993. [Online]. Available: http://books.google.co.jp/books?id=TaIQAQAAMAAJ

[5] C. Wright, A. Buchan, B. Brown, J. Geist, M. Schwerin, D. Rollinson, M. Tesch, and H. Choset, "Design and architecture of the unified modular snake robot," in *ICRA*. IEEE, 2012, pp. 4347–4354.

[6] J. Borenstein, M. Hansen, and A. Borrell, "The omnitread ot-4 serpentine robot - design and performance." *J. Field Robotics*, vol. 24, no. 7, pp. 601–621, 2007.

[7] H. Yamada and S. Hirose, "Development of practical 3-dimentinal active cord mechanism acm-r4," *Journal of Robotics and Mechatronics*, vol. 18, no. 3, pp. 305–311, 2006.

[8] T. Shunichi, Y. Hiroya, and H. Shigeo, "Snake-like active wheel robot acm-r4.1 with joint torque sensor and limiter." in *IROS*. IEEE, 2011, pp. 1081–1086.

[9] K. Kouno, H. Yamada, and S. Hirose, "Development of active-joint active-wheel high traversability snake-like robot acm-r4.2," *Journal of Robotics and Mechatronics*, vol. 25, no. 3, pp. 559–566, 2013.

[10] E. Rohmer, T. Yoshida, K. Ohno, K. Nagatani, S. Tadokoro, and E. Koyanagi, "Quince: A collaborative mobile robotic platform for rescue robots research and development," in *ICAM*, 2010, pp. 225–230.

[11] B. Yamauchi, "Packbot: A versatile platform for military robotics," in *Proceedings of SPIE 5422*, 2004, pp. 228–237.

[12] T. Uehara and Y. Yuguchi, "Development of the quadrupedal walking robot for disaster research and restoration work(saigaijichousa,fukkyusagyouyou yonsokuhokourobotto no kaihatsu)," *Electrical Review*, vol. 98, no. 6, pp. 28–33, jun 2013. [Online]. Available: http://ci.nii.ac.jp/naid/40019704248/

[13] N. Michael, S. Shen, K. Mohta, Y. Mulgaonkar, V. Kumar, K. Nagatani, Y. Okada, S. Kiribayashi, K. Otake, K. Yoshida, K. Ohno, E. Takeuchi, and S. Tadokoro, "Collaborative mapping of an earthquake-damaged building via ground and aerial robots," *J. Field Robot.*, vol. 29, no. 5, pp. 832–841, Sep. 2012. [Online]. Available: http://dx.doi.org/10.1002/rob.21436

[14] H. Yamada and S. Hirose, "Study of active cord mechanism □ approximations to continuous curves of a multi-joint body □ ," *Journal of the robotics society of japan*, vol. 26, no. 1, pp. 110–120, 2008.